HHS Public Access

Author manuscript

DNA Repair (Amst). Author manuscript; available in PMC 2017 July 01.

Published in final edited form as:

DNA Repair (Amst). 2016 July ; 43: 9–17. doi:10.1016/j.dnarep.2016.04.007.

Human DNA polymerase ε is phosphorylated at serine-1940 after DNA damage and interacts with the iron-sulfur complex chaperones CIAO1 and MMS19

Tatiana Moiseeva[1], **Armin M. Gamper**[1,2], **Brian Hood**[3], **Thomas P. Conrads**[3], and **Christopher J. Bakkenist**[1,4,*]

[1]Department of Radiation Oncology, University of Pittsburgh School of Medicine, Hillman Cancer Center, Research Pavilion, Suite 2.6, 5117 Centre Avenue, Pittsburgh, PA 15213-1863, USA

[2]Department of Oncology, University of Alberta, Cross Cancer Institute, 11560 University Avenue, Edmonton, AB T6G 1Z2, Canada

[3]Women's Health Integrated Research Center at Inova Health System, Department of Defense Gynecologic Cancer Center of Excellence, Annandale, VA 22003, USA

[4]Department of Pharmacology and Chemical Biology, University of Pittsburgh School of Medicine, Hillman Cancer Center, Research Pavilion, Suite 2.6, 5117 Centre Avenue, Pittsburgh, PA 15213-1863, USA

Abstract

We describe a dynamic phosphorylation on serine-1940 of the catalytic subunit of human Pol ε, POLE1, following DNA damage. We also describe novel interactions between POLE1 and the iron-sulfur cluster assembly complex CIA proteins CIAO1 and MMS19. We show that serine-1940 is essential for the interaction between POLE1 and MMS19, but not POLE1 and CIAO1. No defect in either proliferation or survival was identified when POLE1 serine-1940 was mutated to alanine in human cells, even following treatment with DNA damaging agents. We conclude that serine-1940 phosphorylation and the interaction between serine-1940 and MMS19 are not essential functions in the C terminal domain of the catalytic subunit of DNA polymerase ε.

INTRODUCTION

Genetic and biochemical studies have suggested that DNA polymerase epsilon (Pol ε) is the major replicative polymerase responsible for the synthesis of the leading strand in eukaryotes [1, 2]. Recent data, however, suggest that DNA polymerase delta (Pol δ) has a major role in the replication of both the leading and lagging DNA strands and that Pol ε has

*To whom correspondence should be addressed: Telephone: (412) 623-7765; FAX: (412) 623-7761; bakkenistcj@upmc.edu.

AUTHOR CONRIBUTIONS

TM completed the experiments. AMG generated essential reagents. BH completed the proteomics analyses. TM, TPC, and CJB designed the experiments and analyzed the data. TM, AMG, TPC and CJB wrote the manuscript.

an important role as a proofreading exonuclease in the removal of Pol δ-generated errors from the leading strand [3]. Pol ε has four subunits that have no homologues in bacteria [4]. The N-terminal half of the largest subunit on Pol ε, POLE1 or p261 in humans and Pol2 in yeast, contains functionally characterized DNA polymerase and 3′-5′ exonuclease domains that are well conserved among eukaryotes [5]. The N-terminal half of Pol2 contains an iron-sulfur cluster that is required for DNA polymerase, but not exonuclease, activity [6]. The C-terminal half of Pol2 contains no experimentally characterized domains aside from two putative Zn-finger modules at the end of the sequence that are conserved from yeast to humans and required for interaction with the second subunit [7, 8]. Remarkably, and somewhat paradoxically, the C-terminal half of Pol2, and 20 amino acids between the two zinc fingers, are essential for viability, while the N-terminal catalytic domain is dispensable in both *S. cerevisiae* and *S. pombe* [7, 9]. The second subunit of Pol ε (POLE2 in humans and Dpb2 in yeast), also called the "B subunit," is essential for viability [10]. The small POLE3 or Dpb3 and POLE4 or Dpb4 subunits of Pol ε bind double-stranded DNA, possibly aiding processivity, but are not essential in *S. cerevisiae* [11].

In addition to its role in DNA replication, Pol ε has been implicated in DNA repair. Genetic analysis of *S. cerevisiae* identified mutations in the PCNA-interacting motif of Pol2 that increased sensitivity to the alkylating agent methyl methanesulfonate (MMS) without impacting DNA replication [12]. Genetic evidence in budding yeast also supports a role for Pol ε in DNA double-strand break (DSB) repair [13], base-excision repair [14], and S phase cell cycle checkpoint activation [15]. Finally, human Pol ε has been shown to function in nucleotide excision repair *in vitro* [16], and has been purified as a component of a large complex that catalyzes homology directed repair of DSBs *in vitro* [17].

DNA damage signaling to POLE1 was identified previously. Phosphorylation of POLE1 serine-1940 was identified in two unbiased proteomics screens for substrates of the apical DNA damage signaling kinases ATM and ATR [18, 19]. Since this phosphorylation is in the essential C-terminal half of POLE1, we speculated that modification of serine-1940 in POLE1 might be functionally significant. We generated antisera that recognize POLE1 only when it is phosphorylated on serine-1940. We show that ATM kinase-dependent POLE1 serine-1940 phosphorylation is rapidly induced after ionizing radiation (IR) in G1 phase as well as in S-phase cells. Similarly, ATR kinase-dependent POLE1 serine-1940 phosphorylation is rapidly induced after ultraviolet radiation (UV) in G1 phase as well as in S-phase cells. An unbiased analysis of proteins that interacted with POLE1 identified a number of novel interacting proteins including the iron-sulfur cluster chaperones CIAO1 and MMS19 as well as chromatin remodeling proteins. POLE1 serine-1940 is essential for the interaction with MMS19, but not CIAO1, as the POLE1 serine-1940-alanine mutant failed to co-purify with MMS19. We conclude that DNA polymerase ε exists in the cell in two distinct complexes containing iron-sulfur chaperones.

MATERIAL AND METHODS

Genetic constructs

cDNA encoding either *POLE1* or *POLE4* was cloned into a FLAG-HA-pIRES expression vector using Nhe1 and EcoR1, and Nde1 and BamH1 restriction sites, respectively.

Serine-1940 was mutated to alanine by substituting a fragment between BstB1 and Sbf1 restriction sites with a DNA fragment containing the mutation synthesized at Life Technologies.

Cell lines, transfections and synchronization

U2OS and 293T cells were cultured in RPMI (Lonza) and DMEM, respectively, supplemented with 10% FBS, 100 U/ml penicillin and 100 μg/ml streptomycin (Lonza). Cells were transfected using Lipofectamine 2000 reagent (Invitrogen). To generate stable cell lines, U2OS cells were selected with 0.5mg/ml G418. For synchronization, U2OS cells were blocked in S-phase with 2 mM thymidine for 24 h, released for 4 h, and blocked in M-phase with 100 ng/ml nocodazole. G1 phase occurred 6 h and S phase occurred 12h after release from nocodazole. Cells were γ-irradiated in a Shepherd Mark I Model 68 [^{137}Cs] irradiator (J.L. Shepherd & Associates) at a dose rate of 0.711 Gy/min.

Antibodies

Antisera against DNA polymerase ε catalytic subunit, POLE1 ([EPR6299] ab134941, Abcam), ATM phospho-S1981 (EP1890Y, Epitomics), generic ATM (A1106, Sigma-Aldrich), Chk1 phospho-S345 (#2348S, Cell Signaling Technology), generic Chk1 (#2360, Cell Signaling Technology), CIAO1 (#81376, Cell signaling), GAPDH (ab9483, Abcam), Geminin (sc-13015, Santa Cruz), MMS19 (ab188156, Abcam), and HA (Clone 12CA5) were used in this study.

Novel antiserum against POLE1 serine-1940 phosphorylation was generated by Rockland Immunochemicals. The peptide GLQD[pS]QKAGGA was synthesized and conjugated to keyhole limpet hemocyanin (KLH). Pre-bleeds from six rabbits were taken before intradermal immunization with the conjugated peptide in Freund's complete adjuvant. Intradermal booster injections were given at day 7 and subcutaneous booster injections were given at days 14, 28 all in Freud's incomplete adjuvant. For the antiserum used throughout these studies, an additional subcutaneous booster injection was given at day 108. Production bleeds and ELISA were performed against both phosphopeptide and nonphosphopeptide at days 38 and 101 and a terminal bleed was performed at day 115. The ratio of the ELISA titer phosphopeptide:nonphosphopeptide was 17 for the serum obtained from the terminal bleed. This antiserum was affinity purified against protein A/G.

Western blotting and immunoprecipitation

Cells were lysed in lysis buffer (50 mM Tris–HCl, pH 7.5, 150 mM NaCl, 50 mM NaF, 0.5% Tween-20, 1% NP40 and 1×protease inhibitor mixture (Roche)) for 20 min on ice. cOmplete Mini, EDTA-free (11 836 170 001) protease inhibitor cocktail tablets were purchased and 1 tablet was used in 10 ml of lysis buffer as directed by the manufacturer. Each tablet is Lysates were cleared by centrifugation, and soluble protein was denatured at 96°C for 10 min in 1× Laemmli sample buffer. For immunoprecipitation, soluble protein extracts were incubated with M2-agarose beads (Sigma) at 4°C for 150 min. Beads were washed 5 times with lysis buffer. Bound proteins were eluted at 96°C for 10 min in 1× Laemmli sample buffer or by incubating protein-bead complexes for 120 min at 4°C in 100

nM FLAG peptide. Proteins were resolved in 4-12% Bis-Tris or 3-8% Tris-acetate gels (Life Technologies), transferred to 0.4 um nitrocellulose membrane (Biorad) and immunoblotted.

In vitro polymerase reaction

dT_{16} primer was 5′ labeled with [γ^{32}P]ATP (3000 Ci/mmol) (PerkinElmer Life sciences) using OptiKinase (Affymetrix). Labeled primer was annealed to poly(dA) (Roche) polynucleotide and used in a reaction containing 20mM TrisHCl pH 7.5, 4% glycerol, 0.1mg/ml BSA, 5mM DTT, 8 mM magnesium acetate, 80 μM each deoxynucleotide and equal volumes of the immunoprecipitated enzymes. Reactions were incubated at 30°C, aliquots were taken at the indicated time points and terminated by adding equal volume of stop solution (95% formamide, 5mM EDTA). Products were resolved on 10% denaturing polyacrylamide gel and visualized with Typhoon 9400 phosphoimager.

In-gel Digestion

Immunoprecipitated protein complexes were resolved by denaturing gel electrophoresis (4-15% Mini-PROTEAN TGX gel, Bio-Rad). Gels were stained for 10 min with Coomassie (SimplyBlue SafeStain, Invitrogen, Carlsbad, CA, USA) and six equivalent sized gel slices were excised for each sample and destained in 25 mM ammonium bicarbonate (AMB) and 50% acetonitrile (ACN, Sigma-Aldrich) at ambient temperature. Gel bands were dehydrated in 100% ACN and incubated in 25 mM AMB, 10 mM dithiothreitol (Sigma-Aldrich) at 56 °C for 30 min followed by alkylation with 25 mM AMB, 45 mM iodoacetamide (Sigma-Aldrich) in darkness for 45 min at ambient temperature. Gel slices were dehydrated in 100% ACN and rehydrated with 20 ng/μL sequencing grade modified trypsin (Promega, Madison, WI, USA) in 25 mM AMB on ice for 45 min. Excess trypsin was removed, gel bands were washed with 500 μL of 25 mM AMB, and proteins digested in-gel at 37 °C for 16 h. Tryptic peptides were extracted with 70% ACN, 5% formic acid (Sigma-Aldrich), dried by vacuum centrifugation and stored at −80 °C.

Liquid Chromatography-Tandem Mass Spectrometry

Duplicate injections of each gel band digest were analyzed by nanoflow liquid chromatography (LC) (Easy-nLC, ThermoFisher Scientific Inc.) coupled online with an LTQ Orbitrap Velos mass spectrometer (MS) (ThermoFisher Scientific Inc.). Following system equilibration, each sample was loaded onto a 2-cm reversed-phase (C-18) vented pre-column (ThermoFisher Scientific Inc.) at 2 μL/min for 9 min with mobile phase A (0.1% formic acid in water). Peptides were resolved on a 100 μm I.D. × 360 μm O.D. × 200 mm long capillary column (Polymicro Technologies, Phoenix, AZ, USA) slurry packed in house with 5 μm diameter, 100 Å pore size reversed phase (Magic C18 AQ, Bruker Michrom Bioresources, Auburn, CA, USA) at a constant flow rate of 200 nL/min by development of a linear gradient of 0.5% mobile phase B (0.1% formic acid in acetonitrile) per min for 80 min, which was then elevated to 95% mobile phase B in 10 min. The column was washed for 10 min with 95% mobile phase B and then equilibrated to 100% mobile phase A prior to the next sample injection. The LTQ-Orbitrap Velos MS was configured to collect high resolution (R = 60,000 at *m/z* 400) broadband mass spectra (*m/z* 375-1800) using the lock mass feature for the polydimethylcyclosiloxane ion (*m/z* 445.12002) generated in the electrospray process from which the twenty-most abundant peptide molecular ions

dynamically determined from the MS scan were selected for tandem MS. Mass spectrometric conditions were set as follows: electrospray voltage, 1.7 kV; no sheath and auxiliary gas flow; capillary temperature, 220 °C; S-Lens RF level, 69%. The ion selection threshold for the Orbitrap (MS) was set at 1.0×10^6 with a maximum ion accumulation time of 500 ms. Tandem MS were collected in the high-pressure linear ion trap (MS/MS) with the following settings: ion threshold, 5000; minimum intensity, 3000; maximum ion accumulation time, 25 ms; activation time, 10 ms. Dynamic exclusion (60 s) was utilized to minimize redundant selection of peptides for MS/MS.

Peptide Identification and Spectral Counting

Tandem mass spectra were searched against the UniProt human protein database (downloaded on 02/21/2014, 68,756 sequences) from the Universal Protein Resource (www.uniprot.org) using Mascot Daemon/Server (v.2.3.2/v.2.3, Matrix Science Inc., Boston, MA) using the automatic decoy search option. The data were searched with a precursor mass tolerance of 10 ppm and a fragment ion tolerance of 0.6 Da. Cysteine carbamidomethylation (*m/z* 57.021464) was set as a fixed modification, methionine oxidation (*m/z* 15.994915) and serine, threonine or tyrosine phosphorylation (*m/z* 79.966331) was set as a dynamic modification. A maximum of two missed tryptic cleavages were allowed. Identified peptides were filtered using an ion score cutoff of 33 resulting in a false peptide discovery rate of less than 1% for all peptides identified (determined from an automatic decoy database search). PSMs whose sequence mapped to multiple protein isoforms were grouped as per the principle of parsimony [20]. Protein abundance differences were determined by spectral counting, where the total PSMs identified for a given protein reflect overall abundance [21]. For each paired comparison, statistical analyses for the enrichment of specific proteins among differentially expressed proteins were performed utilizing a z-statistic test on the $\log_2$-transformed spectral count ratios from normalized data. False positives (q values) were estimated using the R package “q value” [22].

Generation of POLE1 serine-1940-alanine knockin cell lines

pGS-gRNA-Cas9-Puro vectors (Genescript) expressing gRNA sequences targeting non-coding sequences of *POLE1* (ATTTCCGGCTCTCGCGAGTC and CGCACTCGCCGCGCCTGACT) and PIRES-*POLE1* vector (wild-type or serine-1940-alanine) were co-transfected into 293T cells using Lipofectamine 2000 reagent (Invitrogen). Transfected cells were selected with 1ul/ml puromycin for 2 days (until all cells in the non-transfected control were dead), and then grown in the regular conditions. Clonal cell lines were generated from single cells and genomic DNA was isolated using PureLink Genomic DNA Mini Kit (Invitrogen). Successful knockout was assessed using PCR on genomic DNA (primers GCGCCTCTTGATGGACGG and GAAGGCGAGGCCCGAAAA), which confirmed that the DNA fragment between the two targeted sequences was excised (illustrated in Figure 5A).

RESULTS

Generation of POLE1 serine-1940 phosphospecific antiserum

To investigate the dynamics of POLE1 serine-1940 phosphorylation [18, 19], we generated phosphospecific antiserum. Serine-1940 is fourteen amino acids from a domain of unknown function (DUF1744) that is highly conserved from yeast to human and five amino acids from a predicted coiled-coil domain (Figure 1A)[23]. Bioinformatics strategies have revealed a DNA polymerase fold for amino acids 1201–2286, suggesting that two polymerase and exonuclease modules exist in the large subunit of Pol ε [23]. However, key catalytic amino acid residues in both the proofreading 3′-5′ exonuclease and DNA polymerase are disrupted in the C-terminal module (that encompasses DUF1744), consistent with the premise that they are inactive [23]. Mutation of cysteines 665, 668 and 677 in Pol2 to serine (cysteines 651, 654 and 663 in POLE1) inactivate polymerase activity and prevent binding of a [4Fe-4S] iron-sulfur cluster [6]. Two putative zinc fingers are conserved in the C-terminal from yeast to man and while mutations that disrupt either of these zinc fingers in S. cerevisiae Pol2 are viable, deletion of twenty amino acids between them is lethal [7]. POLE1 serine-1940 is conserved in mouse and rat where it is serine-1942, but it is not present in other classes (Figure 1B).

The antiserum generated using a peptide with the sequence GLQD[pS]QKAGGA and used throughout these studies identified FLAG-HA-POLE1 immunopurified from 293T cells 1 h after exposure to IR using anti-FLAG M2 agarose beads (Figure 1C). The antiserum did not identify FLAG-HA-POLE1 purified from either mock-irradiated cells or cells treated with the ATM kinase inhibitor Ku55933 [24] prior to irradiation. Furthermore, the antiserum did not recognize FLAG-HA-POLE1 in which serine-1940 was mutated to alanine, purified from cells following any treatment. Thus, the antiserum identified an IR-induced, ATM kinase-dependent phosphorylation on ectopically expressed POLE1. Similarly, the antiserum identified FLAG-HA-POLE1 immunopurified from cells 1 h after treatment with either ultraviolet light (UV) (Figure 1D) or hydroxyurea (HU) (data not shown). The antiserum did not identify FLAG-HA-POLE1 purified from cells treated with the ATR kinase inhibitor ETP-46464 [25] prior to exposure to the DNA damaging agent. Further, the antiserum did not recognize FLAG-HA-POLE1 in which serine-1940 was mutated to alanine purified from cells treated with either UV or HU. Thus, the antiserum identified both UV- and HU-induced, ATR kinase-dependent phosphorylation on ectopically expressed POLE1.

DNA damage-induced phosphorylation of endogenous POLE1 on serine-1940

The serine-1940 phosphospecific antiserum was not able to detect unpurified POLE1 phosphorylated on serine-1940 in immunoblots of whole cell lysates. We therefore expressed FLAG-HA-POLE4 in 293T cells and immunoprecipitated the four subunit Pol ε complex. POLE1 serine-1940 phosphorylation was induced on the endogenous protein by UV and IR (Figure 1E). UV-induced POLE1 serine-1940 phosphorylation was blocked by treatment with the ATR kinase inhibitor ETP-46464 and IR-induced POLE1 serine-1940 phosphorylation was blocked by treatment with the ATM kinase inhibitor Ku55933. Endogenous POLE1 serine-1940 phosphorylation was also induced by MMS, hydrogen peroxide and HU (Figure 1F).

In vitro analysis of DNA polymerase activity in POLE1 mutants

To determine whether serine-1940 phosphorylation regulates POLE1 catalytic activity, we performed *in vitro* DNA polymerase assays using a ^{32}P-labeled oligo(dT) primer and poly(dA) template (Figure 2A). FLAG-tagged wild-type and mutant POLE1 proteins were immunoprecipitated from 293T cells following transient transfection. Immunoblotting was used to determine that the concentrations of POLE1 proteins in the polymerase assays were similar (Figure 2B). Wild-type, phosphorylation-deficient mutant serine-1940-alanine and phosphomimetic mutant serine-1940-aspartic acid POLE1 proteins had similar polymerase activity *in vitro*, while two mutations in the predicted catalytic site (aspartic acid-860-alanine, aspartic acid-862-alanine) completely blocked the ability of POLE1 to extend the ^{32}P-labeled oligo(dT) primer (Figure 2A).

To determine whether the DNA polymerase activity of POLE1 is required for its phosphorylation in response to DNA damage, catalytically inactive POLE1 and control proteins were expressed in 293T cells and the phosphorylation of serine-1940 was assessed by immunoblotting (Figure 2C). The catalytically inactive POLE1 mutant was phosphorylated on serine-1940 with similar kinetics to control POLE1 proteins.

Cell cycle dependence of DNA damage-induced phosphorylation on POLE1 serine-1940

To investigate the cell cycle dependence of POLE1 serine-1940 phosphorylation, we used thymidine and nocodazole blocks to synchronized U2OS cells that stably expressed FLAG-HA-polE1. POLE1 serine-1940 phosphorylation was induced by IR and UV in both G1 and S phase cells (Figure 3A). IR-induced POLE1 serine-1940 phosphorylation was strongly reduced by the ATM kinase inhibitor Ku55933 in both G1 and S phase cells (Figure 3B). UV-induced POLE1 serine-1940 phosphorylation was detectable for 6 h in asynchronous cells (Figure 3C). At 12 h and 24 h after UV, the amount of POLE1 immunoprecipitated decreased. This may be a consequence of POLE1 degradation and/or cell death.

Mass spectrometry survey for POLE1 serine-1940 phosphorylation-interacting proteins

An unbiased screen to identify proteins that interact with POLE1 was undertaken. Whole cell extracts were generated from U2OS cells stably expressing FLAG-HA-POLE1 and POLE1 protein-protein complexes were immunoprecipitated using anti-FLAG M2 agarose. As a control, protein-protein complexes were also immunoprecipitated using anti-FLAG M2 from U2OS cells not expressing FLAG-fusion proteins. Proteins were eluted from the M2 agarose using FLAG peptide. Eluted proteins were resolved by SDS-PAGE and subject to in-gel digestion and mass spectrometry-based identification. Supplemental Spreadsheet 1 lists 1,396 proteins that were identified.

Interactions between POLE1 and POLE2, POLE3 and POLE4 and DNA damage-binding protein 1 (DDB1), the iron-sulfur cluster chaperones CIAO1 and MMS19, and the RNA polymerase II subunit RPB2 are summarized in Table 1. These data show that the ectopically expressed POLE1 protein forms a complex with the smaller endogenous Pol ε proteins. We choose to further investigate novel interactions between POLE1 and DDB1, CIAO1, MMS19 and RPB2 as work in yeast, that has not been extended to human cells previously, showed that POLE1 contains an iron-sulfur cluster [6], and that a protein complex

comprising POLE1/Mms19/Rik1 (a yeast protein related to DDB1)/Dos1/Dos2 is required to recruit RNA polymerase II to DNA [26].

A specific interaction between MMS19 and POLE1 is disrupted in the POLE1 serine-1940-alanine mutant

S. cerevisiae Pol2 was recently shown to contain an iron-sulfur cluster [6]. The iron-sulfur cluster assembly complex CIA comprises CIAO1 and MMS19 [27]. To validate novel interactions between POLE1 and CIAO1 and MMS19, and determine whether these interactions required serine-1940, we immunoblotted immunoprecipitations of FLAG-HA-POLE1 wild-type and POLE1 serine-1940-alanine mutant. MMS19 co-purified with POLE1 wild-type, but not POLE1 serine-1940-alanine mutant (Figure 4A). The interaction between MMS19 and POLE1 wild-type was validated and found to be DNA damage-independent by immunoblotting with MMS19 specific antisera (Figures 4A, B). The interaction between MMS19 and POLE1 wild-type was not an artifact of the two proteins binding DNA as it was not disrupted by either DNAse1 or ethidium bromide (Figure 4C). However, the binding of MMS19 and POLE1 was abolished by POLE1 serine-1940-alanine mutation (Figures 4A, B).

Immunoblotting with CIAO1 specific antisera also corroborated the binding of CIAO1 and POLE1, and this interaction was also found to be DNA damage-independent (Figure 4D). In contrast to the binding of MMS19 and POLE1, POLE1 serine-1940-alanine mutation did not affect the binding of CIAO1 and the DNA polymerase.

POLE1 serine-1940-alanine mutation does not affect cell viability

In order to determine the effect of POLE1 serine-1940-alanine mutation, which disrupts the interaction between POLE1 and MMS19 (Figure 4) but not DNA polymerase activity (Figure 2), on cell proliferation we generated a POLE1 mutant 293T cell line. Endogenous *POLE1* was knocked out using the CRISPR-Cas9 system and wild-type or serine-1940-alanine mutant FLAG-HA-POLE1 was ectopically expressed (Figure 5A). Knock-out efficiency was tested by PCR on genomic DNA (Figure 5B). Cell growth was assayed for the original 293T cell line and two clonal lines with POLE1 wild-type or serine-1940-alanine complementation (Figure 5C). No significant difference in cell growth between the five cell lines was observed. In addition, cell cycle progression was similar in all cell lines (Figure 5D).

To determine whether POLE1 serine-1940-alanine mutation sensitizes 293T cells to DNA damage, cells were irradiated with 3 Gy of IR and counted at 48 h (Figure 5E). No significant difference in survival and proliferation between cells overexpressing POLE1 wild-type or serine-1940-alanine mutation was observed, Interestingly, the parental 293T cell line was the most radiosensitive cell line, suggesting that overexpression of either POLE1 wild-type or serine-1940-alanine is radioprotective and that serine-1940-alanine mutation does not impact the mechanism(s) underlying the observed radioprotection.

DISCUSSION

We describe a dynamic phosphorylation on serine-1940 of the catalytic subunit of human Pol ε, POLE1, following DNA damage. We also describe novel interactions between POLE1 and the iron-sulfur cluster assembly complex CIA proteins CIAO1 and MMS19 [27]. We show that serine-1940 is essential for the interaction between POLE1 and MMS19, but not POLE1 and CIAO1. No defect in either proliferation or survival was identified when POLE1 serine-1940 was mutated to alanine in human cells, even following treatment with DNA damaging agents.

A dynamic phosphorylation on POLE1 serine-1940 of human Pol ε

We have characterized a dynamic phosphorylation on serine-1940 of the catalytic subunit of human Pol ε, POLE1, that is rapidly induced by all DNA damaging agents tested and that persists for at least 6 h following exposure to UV. POLE1 serine-1940 phosphorylation is ATM kinase-dependent following IR, and ATR kinase-dependent following UV and HU. DNA damage-induced POLE1 serine-1940 phosphorylation is observed in both G1 and S phase cells. Since Pol ε was previously found to be associated with chromatin throughout the cell cycle [28], and ATR kinase activity can be induced also in G1 phase cells [29], this may simply be a consequence of the proximity of active ATM and/or ATR with Pol ε. We have argued previously that many phosphorylations catalyzed by ATM and/or ATR kinase after DNA damage may have no or redundant function [30]. Consistent with this premise, we show that POLE1 phosphorylation neither changes nor requires the DNA polymerase activity of POLE1.

An interaction between Pol ε and iron-sulfur cluster chaperones

We provide the first experimental evidence that human Pol ε interacts with the iron-sulfur cluster chaperone proteins CIAO1 and MMS19. The large subunit of *S. cerevisiae* Pol ε itself was recently found to contain an iron-sulfur cluster [6]. The iron-sulfur cluster (4Fe-4S) in POLE1 is coordinated by a cysteine-rich insertion in the active DNA polymerase domain in the N-terminal half of the protein and is essential for DNA polymerase, but not exonuclease activity, in the purified protein. This iron-sulfur cluster in POLE1 appears to be functionally distinct to the iron-sulfur clusters identified in the C-terminal metal-binding domains (CTD) of Pol δ and Pol ζ [31], which have a structural role in protein-protein complex assembly. While two putative zinc finger proteins were described in the C-terminal domain of POLE1, [7] there is uncertainty as to whether these zinc fingers bind zinc or iron [31]. Biochemical purification of POLE1 with the iron-sulfur cluster used a protein that lacked the C-terminal, cysteine rich domain [6]. Based on the conservation between the CTDs in Pol δ and Pol ζ and Pol ε, POLE1 may bind a second iron-sulfur cluster.

Iron-sulfur clusters are assembled in the mitochondria, they do not form spontaneously [32]. After synthesis in the mitochondria, iron-sulfur clusters are exported to the cytoplasm, where a protein complex that includes CIAO1 and MMS19 transfers iron-sulfur clusters to target proteins essential for genome stability [33-35]. Disruption of MMS19 causes nuclear genome instability and our finding that MMS19 binds POLE1, is consistent with the premise that MMS19 is required for the assembly of an iron-sulfur cluster in the POLE1.

Mutation of cysteines 665, 668 and 677 to serine in *S. cerevisiae* Pol2 inactivates polymerase activity and prevents binding of a [4Fe-4S] iron-sulfur cluster [6]. However, mutation of serine-1940 to alanine in POLE1 prevents MMS19 binding but does not impact kinase activity *in vitro*. It is possible that the interaction between POLE1 and MMS19 is not essential for the assembly of the iron-sulfur cluster in the N-terminal half of POLE1. It is also possible that the mutations that disrupt the binding of the iron-sulfur cluster in *S. cerevisiae* disrupt DNA polymerase activity through another mechanism. It is important to know whether the N-terminal iron-sulfur cluster is essential for DNA polymerase activity as the sensitivity of iron-sulfur clusters to oxidation may provide a means to couple DNA synthesis and repair by Pol ε to oxidative stress in eukaryotic cells. It has been hypothesized previously that Pol ε may be more sensitive to changes in oxidative stress than other DNA polymerases in eukaryotic cells as it contains an iron-sulfur cluster in the DNA polymerase catalytic domain [36].

A novel CIAO1 complex

CIAO1 has been identified in two complexes. First, the iron-sulfur cluster assembly complex CIA comprises CIAO1 and Mms19 [27]. Second, the MMXD complex (important for chromosome segregation during mitosis) comprises CIAO1, Mms19 and XPD, and is thought to stabilize an iron-sulfur cluster in XPD [37]. The interactions between CIAO1 and POLE1, and MMS19 and POLE1, were not changed following DNA damage, which suggests that they function in iron-sulfur cluster assembly in unstressed as well as stressed conditions. However, we have shown that POLE1 serine 1940 is essential for the interaction of DNA polymerase ε with MMS19, but redundant for CIAO1 binding to DNA polymerase ε This indicates that CIAO1 can bind POLE1 in the absence of MMS19 and that a CIAO1 complex, besides the previously described MMXD and CIA complexes, exists in the cell.

Supplementary Material

Refer to Web version on PubMed Central for supplementary material.

ACKNOWLEDGEMENTS

We thank Dr. Patricia Opresko and Justin Lormand for their help with the *in vitro* DNA polymerase activity assay.

FUNDING

This work was supported by NIH Grants RO1 CA148644 and P50 CA090440 Project 4 to CJB, and UM1 CA186690 and P30 CA047904.

REFERENCES

[1]. Pursell ZF, Isoz I, Lundstrom EB, Johansson E, Kunkel TA. Yeast DNA polymerase epsilon participates in leading-strand DNA replication. Science. 2007; 317:127–130. [PubMed: 17615360]

[2]. Langston LD, Zhang D, Yurieva O, Georgescu RE, Finkelstein J, Yao NY, Indiani C, O'Donnell ME. CMG helicase and DNA polymerase epsilon form a functional 15-subunit holoenzyme for eukaryotic leading-strand DNA replication. Proceedings of the National Academy of Sciences of the United States of America. 2014; 111:15390–15395. [PubMed: 25313033]

[3]. Johnson RE, Klassen R, Prakash L, Prakash S. A Major Role of DNA Polymerase delta in Replication of Both the Leading and Lagging DNA Strands. Molecular cell. 2015; 59:163–175. [PubMed: 26145172]

[4]. Pursell ZF, Kunkel TA. DNA polymerase epsilon: a polymerase of unusual size (and complexity). Progress in nucleic acid research and molecular biology. 2008; 82:101–145. [PubMed: 18929140]

[5]. Burgers PM, Bambara RA, Campbell JL, Chang LM, Downey KM, Hubscher U, Lee MY, Linn SM, So AG, Spadari S. Revised nomenclature for eukaryotic DNA polymerases. European journal of biochemistry / FEBS. 1990; 191:617–618. [PubMed: 2390988]

[6]. Jain R, Vanamee ES, Dzikovski BG, Buku A, Johnson RE, Prakash L, Prakash S, Aggarwal AK. An iron-sulfur cluster in the polymerase domain of yeast DNA polymerase epsilon. Journal of molecular biology. 2014; 426:301–308. [PubMed: 24144619]

[7]. Dua R, Levy DL, Campbell JL. Role of the putative zinc finger domain of Saccharomyces cerevisiae DNA polymerase epsilon in DNA replication and the S/M checkpoint pathway. The Journal of biological chemistry. 1998; 273:30046–30055. [PubMed: 9792727]

[8]. Jaszczur M, Flis K, Rudzka J, Kraszewska J, Budd ME, Polaczek P, Campbell JL, Jonczyk P, Fijalkowska IJ. Dpb2p, a noncatalytic subunit of DNA polymerase epsilon, contributes to the fidelity of DNA replication in Saccharomyces cerevisiae. Genetics. 2008; 178:633–647. [PubMed: 18245343]

[9]. Feng W, D'Urso G. Schizosaccharomyces pombe cells lacking the amino-terminal catalytic domains of DNA polymerase epsilon are viable but require the DNA damage checkpoint control. Molecular and cellular biology. 2001; 21:4495–4504. [PubMed: 11416129]

[10]. Isoz I, Persson U, Volkov K, Johansson E. The C-terminus of Dpb2 is required for interaction with Pol2 and for cell viability. Nucleic acids research. 2012; 40:11545–11553. [PubMed: 23034803]

[11]. Li Y, Pursell ZF, Linn S. Identification and cloning of two histone fold motif-containing subunits of HeLa DNA polymerase epsilon. The Journal of biological chemistry. 2000; 275:31554. [PubMed: 11013269]

[12]. Dua R, Levy DL, Li CM, Snow PM, Campbell JL. In vivo reconstitution of Saccharomyces cerevisiae DNA polymerase epsilon in insect cells. Purification and characterization. The Journal of biological chemistry. 2002; 277:7889–7896. [PubMed: 11756442]

[13]. Holmes AM, Haber JE. Double-strand break repair in yeast requires both leading and lagging strand DNA polymerases. Cell. 1999; 96:415–424. [PubMed: 10025407]

[14]. Wang Z, Wu X, Friedberg EC. DNA repair synthesis during base excision repair in vitro is catalyzed by DNA polymerase epsilon and is influenced by DNA polymerases alpha and delta in Saccharomyces cerevisiae. Molecular and cellular biology. 1993; 13:1051–1058. [PubMed: 8423775]

[15]. Navas TA, Zhou Z, Elledge SJ. DNA polymerase epsilon links the DNA replication machinery to the S phase checkpoint. Cell. 1995; 80:29–39. [PubMed: 7813016]

[16]. Shivji MK, Podust VN, Hubscher U, Wood RD. Nucleotide excision repair DNA synthesis by DNA polymerase epsilon in the presence of PCNA, RFC, and RPA. Biochemistry. 1995; 34:5011–5017. [PubMed: 7711023]

[17]. Jessberger R, Podust V, Hubscher U, Berg P. A mammalian protein complex that repairs double-strand breaks and deletions by recombination. The Journal of biological chemistry. 1993; 268:15070–15079. [PubMed: 8392064]

[18]. Olsen JV, Vermeulen M, Santamaria A, Kumar C, Miller ML, Jensen LJ, Gnad F, Cox J, Jensen TS, Nigg EA, Brunak S, Mann M. Quantitative phosphoproteomics reveals widespread full phosphorylation site occupancy during mitosis. Science signaling. 2010; 3:ra3. [PubMed: 20068231]

[19]. Matsuoka S, Ballif BA, Smogorzewska A, McDonald ER 3rd, Hurov KE, Luo J, Bakalarski CE, Zhao Z, Solimini N, Lerenthal Y, Shiloh Y, Gygi SP, Elledge SJ. ATM and ATR substrate analysis reveals extensive protein networks responsive to DNA damage. Science. 2007; 316:1160–1166. [PubMed: 17525332]

[20]. Marengo E, Robotti E, Bobba M, Gosetti F. The principle of exhaustiveness versus the principle of parsimony: a new approach for the identification of biomarkers from proteomic spot volume datasets based on principal component analysis. Anal Bioanal Chem. 2010; 397:25–41. [PubMed: 20091299]

[21]. Liu H, Sadygov RG, Yates JR 3rd. A model for random sampling and estimation of relative protein abundance in shotgun proteomics. Analytical Chemistry. 2004; 76:4193–4201. [PubMed: 15253663]

[22]. Storey JD, Tibshirani R. Statistical significance for genomewide studies. Proceedings of the National Academy of Sciences of the United States of America. 2003; 100:9440–9445. [PubMed: 12883005]

[23]. Tahirov TH, Makarova KS, Rogozin IB, Pavlov YI, Koonin EV. Evolution of DNA polymerases: an inactivated polymerase-exonuclease module in Pol epsilon and a chimeric origin of eukaryotic polymerases from two classes of archaeal ancestors. Biology direct. 2009; 4:11. [PubMed: 19296856]

[24]. Hickson I, Zhao Y, Richardson CJ, Green SJ, Martin NM, Orr AI, Reaper PM, Jackson SP, Curtin NJ, Smith GC. Identification and characterization of a novel and specific inhibitor of the ataxia-telangiectasia mutated kinase ATM. Cancer research. 2004; 64:9152–9159. [PubMed: 15604286]

[25]. Toledo LI, Murga M, Zur R, Soria R, Rodriguez A, Martinez S, Oyarzabal J, Pastor J, Bischoff JR, Fernandez-Capetillo O. A cell-based screen identifies ATR inhibitors with synthetic lethal properties for cancer-associated mutations. Nature structural & molecular biology. 2011; 18:721–727.

[26]. Li F, Martienssen R, Cande WZ. Coordination of DNA replication and histone modification by the Rik1-Dos2 complex. Nature. 2011; 475:244–248. [PubMed: 21725325]

[27]. Balk J, Aguilar Netz DJ, Tepper K, Pierik AJ, Lill R. The essential WD40 protein Cia1 is involved in a late step of cytosolic and nuclear iron-sulfur protein assembly. Molecular and cellular biology. 2005; 25:10833–10841. [PubMed: 16314508]

[28]. Vaara M, Itkonen H, Hillukkala T, Liu Z, Nasheuer HP, Schaarschmidt D, Pospiech H, Syvaoja JE. Segregation of replicative DNA polymerases during S phase: DNA polymerase epsilon, but not DNA polymerases alpha/delta, are associated with lamins throughout S phase in human cells. The Journal of biological chemistry. 2012; 287:33327–33338. [PubMed: 22887995]

[29]. Gamper AM, Rofougaran R, Watkins SC, Greenberger JS, Beumer JH, Bakkenist CJ. ATR kinase activation in G1 phase facilitates the repair of ionizing radiation-induced DNA damage. Nucleic acids research. 2013; 41:10334–10344. [PubMed: 24038466]

[30]. Choi S, Bakkenist CJ. Brd4 shields chromatin from ATM kinase signaling storms. Science signaling. 2013; 6:pe30. [PubMed: 24045152]

[31]. Netz DJ, Stith CM, Stumpfig M, Kopf G, Vogel D, Genau HM, Stodola JL, Lill R, Burgers PM, Pierik AJ. Eukaryotic DNA polymerases require an iron-sulfur cluster for the formation of active complexes. Nature chemical biology. 2012; 8:125–132. [PubMed: 22119860]

[32]. Lill R, Muhlenhoff U. Maturation of iron-sulfur proteins in eukaryotes: mechanisms, connected processes, and diseases. Annual review of biochemistry. 2008; 77:669–700.

[33]. Stehling O, Vashisht AA, Mascarenhas J, Jonsson ZO, Sharma T, Netz DJ, Pierik AJ, Wohlschlegel JA, Lill R. MMS19 assembles iron-sulfur proteins required for DNA metabolism and genomic integrity. Science. 2012; 337:195–199. [PubMed: 22678362]

[34]. Gari K, Leon Ortiz AM, Borel V, Flynn H, Skehel JM, Boulton SJ. MMS19 links cytoplasmic iron-sulfur cluster assembly to DNA metabolism. Science. 2012; 337:243–245. [PubMed: 22678361]

[35]. Veatch JR, McMurray MA, Nelson ZW, Gottschling DE. Mitochondrial dysfunction leads to nuclear genome instability via an iron-sulfur cluster defect. Cell. 2009; 137:1247–1258. [PubMed: 19563757]

[36]. Fuss JO, Tsai CL, Ishida JP, Tainer JA. Emerging critical roles of Fe-S clusters in DNA replication and repair. Biochimica et biophysica acta. 2015; 1853:1253–1271. [PubMed: 25655665]

[37]. Ito S, Tan LJ, Andoh D, Narita T, Seki M, Hirano Y, Narita K, Kuraoka I, Hiraoka Y, Tanaka K. MMXD, a TFIIH-independent XPD-MMS19 protein complex involved in chromosome segregation. Molecular cell. 2010; 39:632–640. [PubMed: 20797633]

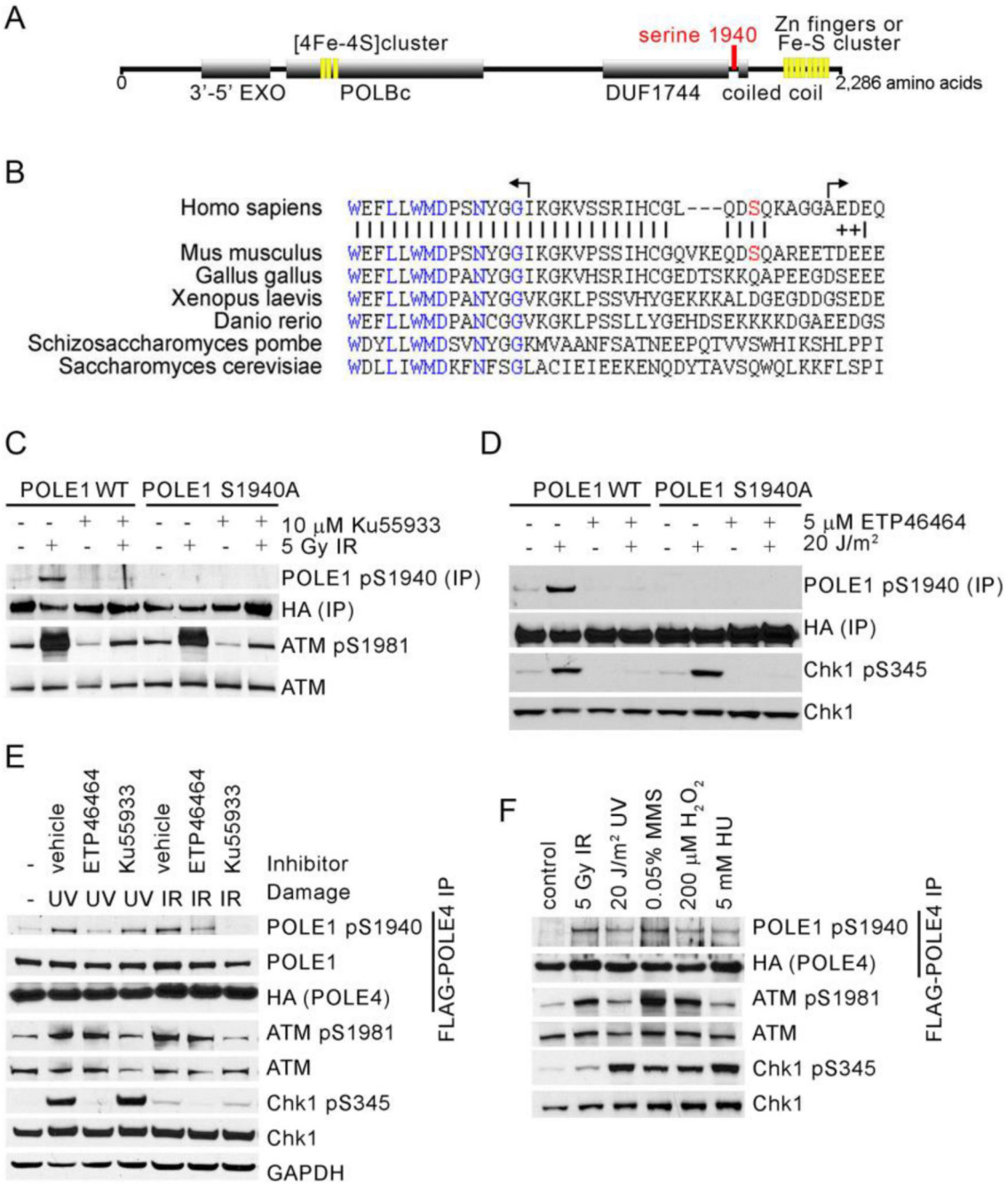

Figure 1. POLE1 is phosphorylated on serine-1940 by ATM and ATR after DNA damage

A. Structure of the catalytic subunit of DNA polymerase ε, POLE1. **B**. Sequence alignment of POLE1 around S1940. **C/D.** FLAG-HA-POLE1 wild-type (WT) and S1940A mutant (SA) were expressed in 293T cells. ATM (Ku55933) or ATR (ETP46464) kinase inhibitor was added to cells 15 minutes prior to exposure to 5Gy IR (C) or 20 J/m^2 UV (D). Cells were harvested 1h later and FLAG-tagged POLE1 was immunoprecipitated using M2-agarose beads. ATM or Chk1 phosphorylation were immunoblotted as controls for DNA damage and ATM and ATR kinase inhibitors. **E/F.** FLAG-HA-tagged POLE4 was expressed

in 293T cells. Cells were exposed to 5Gy IR or 20 J/m^2 UV (E) or 0.05% methylmethanesulfonate (MMS), 200 μM hydrogen peroxide (H2O2) or 5 mM hydroxyurea (HU) (F). Cells were harvested 1h later and FLAG-tagged POLE4 was immunoprecipitated using M2-agarose beads.

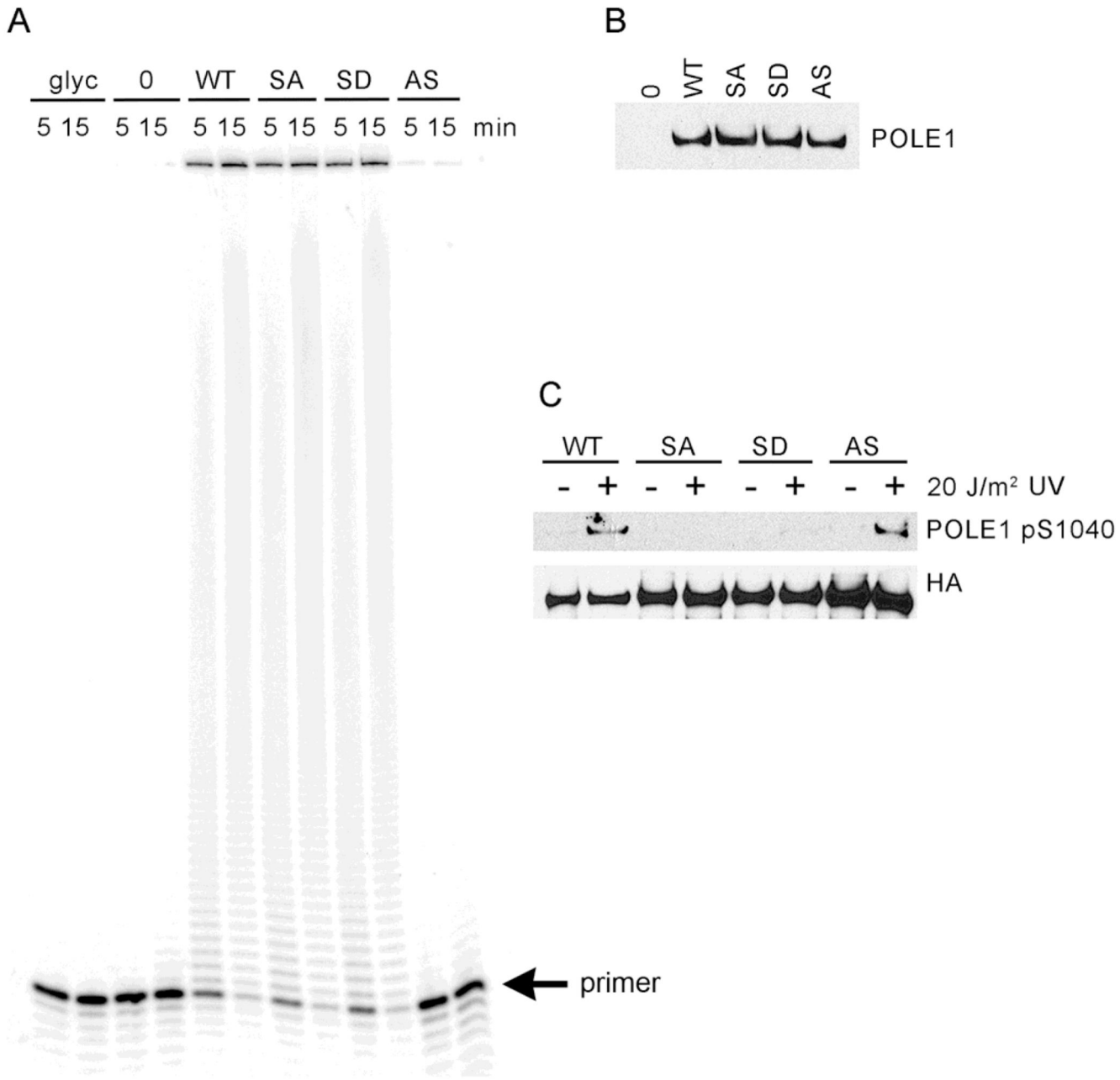

Figure 2. Mutations at S1940 do not affect the DNA polymerase activity of POLE1 *in vitro*

A. FLAG-HA-POLE1 WT, S1940A (SA), S1940D (SD), and catalytic inactive D860, 862A (AS) mutants were expressed in 293T cells. FLAG-tagged POLE1 was immunoprecipitated using M2-agarose beads. DNA synthesis catalyzed by each immunoprecipitation in an *in vitro* primer extension from alpha^{32}P-labeled dT16 primer on a poly(dA) template at 5 and 15 minutes is shown. The position of the primer is indicated. Glycerol and mock-IP from 293T cells were used as negative controls. **B.** Immunoblots using anti-POLE1 antisera ensured similar concentrations of POLE1 were used in the primer extension assay. **C.** FLAG-HA-POLE1 WT, S1940A (SA), S1940D (SD), and catalytic inactive D860, 862A

(AS) mutants were expressed in 293T cells. Cells were exposed to 10 J/m^2 UV. Cells were harvested 1h later and FLAG-tagged POLE1 was immunoprecipitated using M2-agarose beads. FLAG-HA-POLE1 was identified using anti-HA (Clone 12CA5).

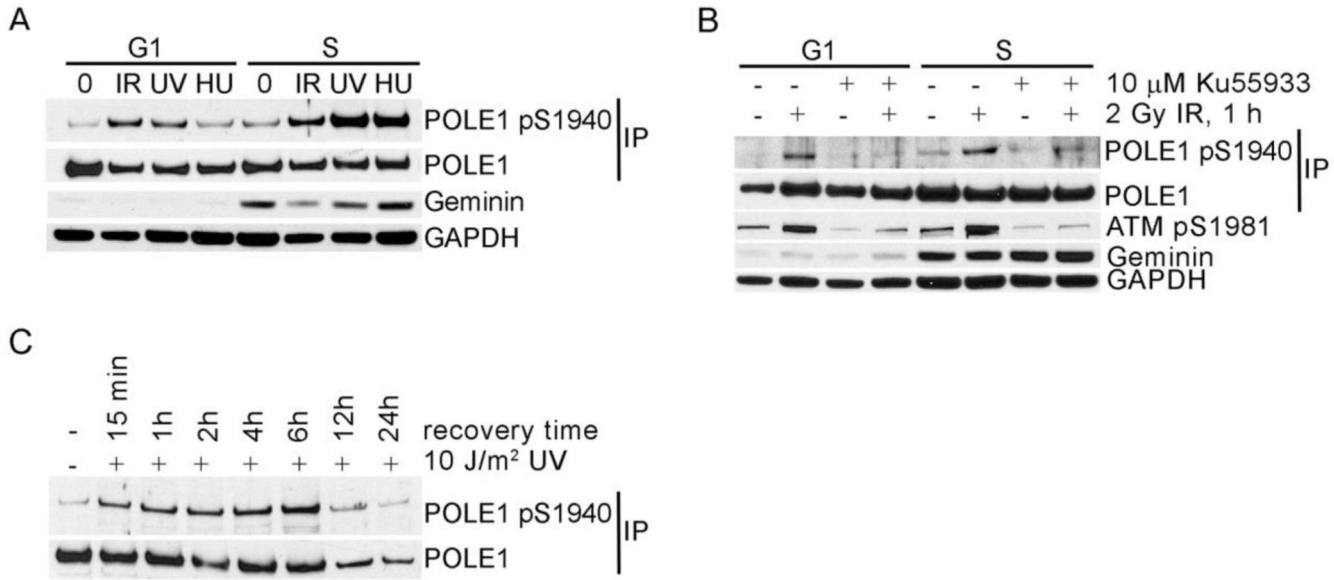

Figure 3. POLE1 is phosphorylated after DNA damage in G1 as well as in S-phase cells

A/B. U2OS cells stably expressing FLAG-HA-POLE1 were synchronized in G1 phase using a double thymidine-nocodazol block. Following release, cells in G1 or S-phase were exposed to 2Gy IR, 20 J/m^2 UV, or 5mM HU (A) or treated with Ku55933 15 minutes prior to 2Gy IR (B). Cells were harvested 1h later and FLAG-tagged POLE1 was immunoprecipitated using M2-agarose beads. Geminin was immunoblotted as a control for synchronization. **C.** Asynchronous U2OS cells, stably expressing FLAG-HA-POLE1 were exposed to 10 J/m^2 UV and FLAG-tagged POLE1 was immunoprecipitated using M2-agarose beads at the time-points indicated.

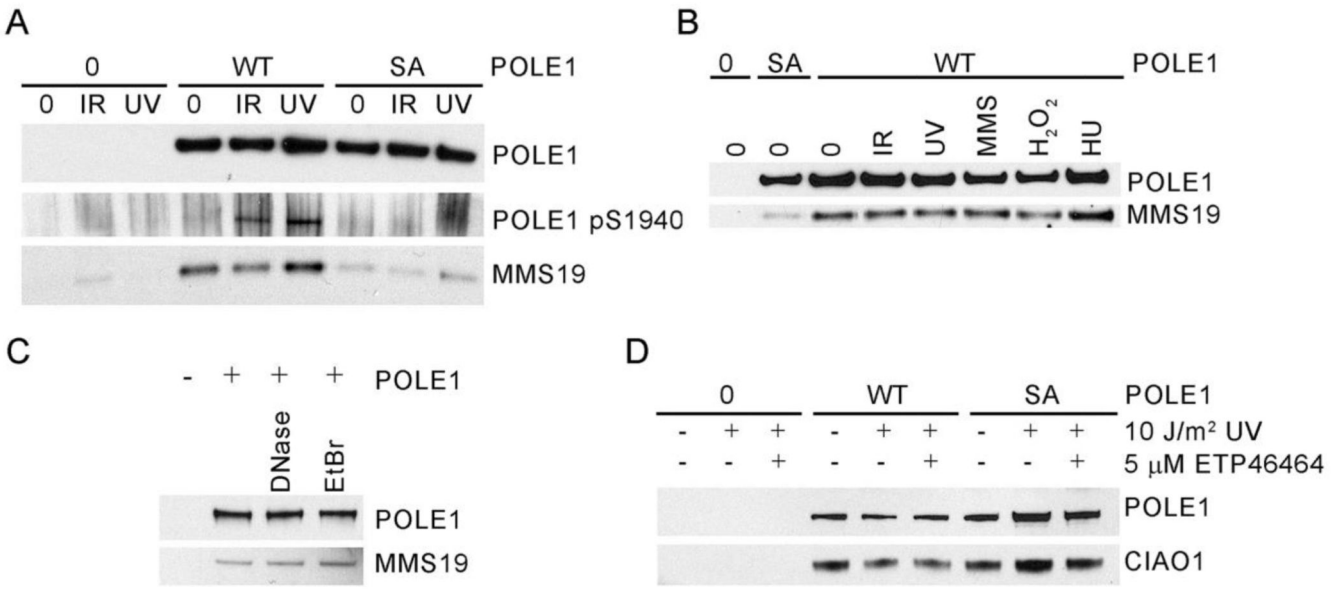

Figure 4. POLE1 interacts with MMS19 and CIAO1

A/B. U2OS cells stably expressing FLAG-HA-POLE1 WT or S1940A mutant were treated with 2 Gy IR or 10 J/m^2 UV (A), and 2Gy IR, 10 J/m^2 UV, 0.05% MMS, 200 μM H_2O_2 or 5mM HU (B). Cells were harvested 1h later and FLAG-tagged POLE1 was immunoprecipitated using M2-agarose beads. Proteins were eluted using FLAG-peptide. **C.** U2OS cells stably expressing FLAG-HA-POLE1 WT were harvested and 100 units of DNAse I or 20 μg/ml eithidium bromide (EtBr) were added to lysates prior to immunoprecipitation to disrupt DNA-mediated interactions. **D.** FLAG-HA-POLE1 WT or S1940A were expressed in 293T cells. ATR inhibitor (ETP46464) was added 15 minutes prior to 10 J/m^2 UV. Cells were harvested 1h later and FLAG-tagged POLE1 was immunoprecipitated using M2-agarose beads. Proteins were eluted using FLAG-peptide.

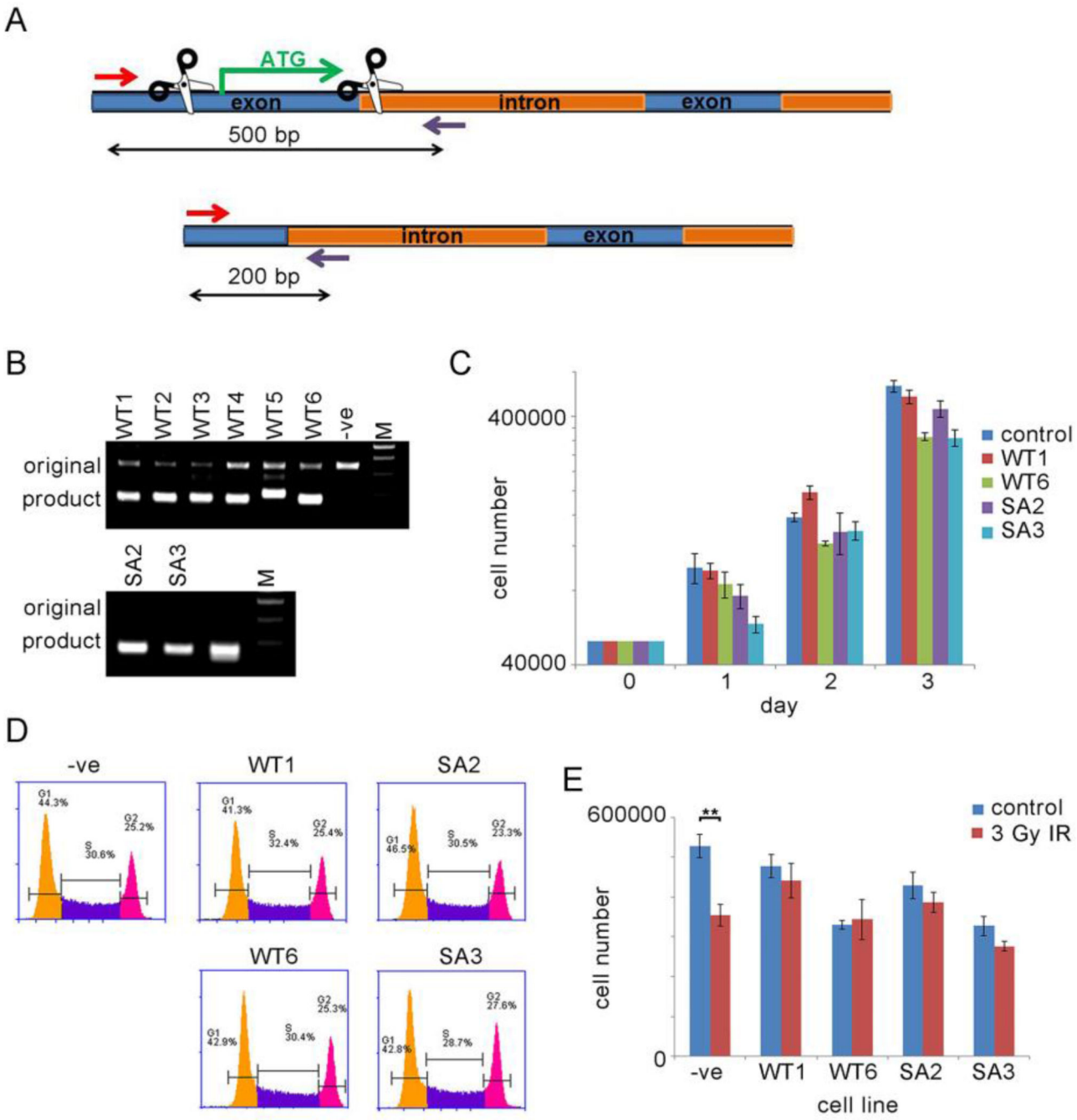

Figure 5. POLE1 S1940A mutation does not affect cell proliferation or sensitivity to DNA damage

A. A schematic of the CRISPR/Cas9-based knock-out and PCR validation strategy. Two gRNAs targeting non-coding sequence of *POLE1* gene were used to excise coding sequence and a splice site. PCR primers were selected to amplify a genomic DNA fragment of ~500bp in the original cell line or ~200bp following successful knock-out (KO). **B.** PCR from the cell lines used complemented with FLAG-HA-POLE1 WT and S1940A mutant. **C.** Cells were seeded at 50 000 and counted in triplicate 24, 48 and 72 h. **D.** Cell cycle profile of

exponentially dividing cells were determined using flow cytometry. **E.** Cells were seeded at 50 000 per plate and irradiated with 3Gy IR at 24 h. Surviving cells were counted in triplicate at 72 h.

Table 1

POLE1 Interacting proteins

POLE1 associated proteins identified by mass spectrometry that are discussed in this study.

Gene Name	UniProt Accession	Number of Peptides
POLE1 (p261)	Q07864	1383
POLE2	P56282	100
POLE3	Q9NRF9	37
POLE4	Q9NR33	19
DDB1	Q16531	17
CIAO1	O76071	19
MMS19	Q96T76	19
RPB2	P30876	9